

Unsupervised Surface Reflectance Field Multi-segmenter

Michal Haindl¹(✉), Stanislav Mikeš¹, and Mineichi Kudo²

¹ The Institute of Information Theory and Automation of the Czech Academy
of Sciences, Prague, Czech Republic

{haindl,xaos}@utia.cz

² Graduate School of Engineering, Hokkaido University, Sapporo, Japan
mine@main.eng.hokudai.ac.jp

Abstract. An unsupervised, illumination invariant, multi-spectral, multi-resolution, multiple-segmenter for textured images with unknown number of classes is presented. The segmenter is based on a weighted combination of several unsupervised segmentation results, each in different resolution, using the modified sum rule. Multi-spectral textured image mosaics are locally represented by eight causal directional multi-spectral random field models recursively evaluated for each pixel. The single-resolution segmentation part of the algorithm is based on the underlying Gaussian mixture model and starts with an over segmented initial estimation which is adaptively modified until the optimal number of homogeneous texture segments is reached. The performance of the presented method is extensively tested on the Prague segmentation benchmark both on the surface reflectance field textures as well as on the static colour textures using the commonest segmentation criteria and compares favourably with several leading alternative image segmentation methods.

Keywords: Unsupervised image segmentation · Textural features · Illumination invariants · Surface reflectance field · Bidirectional texture function

1 Introduction

Segmentation is the fundamental process which partitions a data space into meaningful salient regions. Image segmentation essentially affects the overall performance of any automated image analysis system thus its quality is of the utmost importance. Image regions, homogeneous with respect to some usually textural or colour measure, which result from a segmentation algorithm are analysed in subsequent interpretation steps. Texture-based image segmentation is area of intense research activity in recent years and many algorithms were published in consequence of all this effort. These methods are usually categorised

[18] as region-based, boundary-based, or as a hybrid of the two. Different published methods are difficult to compare because of lack of a comprehensive analysis together with accessible experimental data, however available results indicate that the ill-defined texture segmentation problem is still far from being satisfactorily solved. Spatial interaction models and especially Markov random fields-based models are increasingly popular for texture representation [4, 18], etc. Several researchers dealt with the difficult problem of unsupervised segmentation using these models see for example [10, 15, 17] or [5, 7, 12]. The concept of decision fusion [14] for high-performance pattern recognition is well known and widely accepted in the area of supervised classification where (often very diverse) classification technologies, each providing complementary sources of information about class membership, can be integrated to provide more accurate, robust and reliable classification decisions than the single classifier applications.

Similar advantages can be expected and achieved [12] also for the unsupervised segmentation applications. However, a direct unsupervised application of the supervised classifiers fusion idea is complicated with unknown number of data hidden classes and consequently a different number of segmented regions in segmentation results to be fused. This paper exploits above advantages by combining several unsupervised segmenters of the same type but with different feature sets. It introduces a novel eight-directional generative multispectral texture representation and invariant features capable to discriminate surface reflectance field type of textures, i.e., bidirectional texture function (BTF) textures with a fixed or small range of viewing angle.

2 Combination of Multiple Segmenters

The proposed method (MW3AR8ⁱ) combines segmentation results from different resolution. We assume to down-sample input image Y into M different resolutions $Y^{(m)} = \downarrow^{\iota_m} Y$ with sampling factors ι_m $m = 1, \dots, M$ identical in both horizontal and vertical directions and $Y^{(1)} = Y$. Local surface reflectance field texture for each pixel $Y_r^{(m)}$ in resolution m is represented the 3D simultaneous causal autoregressive random field model (CAR) parameter space $\Theta_r^{(m)}$ (5) and modeled by the Gaussian mixture model (6),(7).

2.1 Single-Resolution Texture Model

Static smooth multi-spectral textures require three dimensional models for adequate representation. We assume that single multi-spectral textures can be locally modelled using a 3D simultaneous causal autoregressive random field model (CAR). This model can be expressed as a stationary causal uncorrelated noise driven 3D autoregressive process [11]:

$$Y_r = \gamma X_r + e_r, \quad (1)$$

where $\gamma = [A_1, \dots, A_\eta]$ is the $d \times d\eta$ parameter matrix, $A_i \forall i \in I_r^c$ are $d \times d$ parametric matrices, d is the number of spectral bands, I_r^c is a causal neighborhood index set with $\eta = \text{card}(I_r^c)$ and e_r is a white Gaussian noise vector

with zero mean and a constant but unknown covariance, X_r is a corresponding vector of the contextual neighbours Y_{r-s} where $s \in I_r^c$ and $r, r-1, \dots$ is a chosen direction of movement on the image index lattice I . The selection of an appropriate CAR model support ($I_r^c \subset I$) is important to obtain good texture representation but less important for segmentation. The optimal neighbourhood as well as the Bayesian parameters estimation of a CAR model can be found analytically under few additional and acceptable assumptions using the Bayesian approach (see details in [11]). The recursive Bayesian parameter estimation of the CAR model is [11]:

$$\hat{\gamma}_{r-1}^T = \hat{\gamma}_{r-2}^T + \frac{V_{x(r-2)}^{-1} X_{r-1} (Y_{r-1} - \hat{\gamma}_{r-2} X_{r-1})^T}{(1 + X_{r-1}^T V_{x(r-2)}^{-1} X_{r-1})}, \quad (2)$$

where $V_{x(r-1)} = \sum_{k=1}^{r-1} X_k X_k^T + V_{x(0)}$. Local texture for each pixel is represented by eight parametric vectors. Each vector contains local estimations of the CAR model parameters. These eight models have identical contextual neighbourhood I_r^c but they differ in their major movement direction ($\downarrow, \uparrow, \rightarrow, \leftarrow, \searrow, \swarrow, \nearrow, \nwarrow$), i.e.,

$$\tilde{\gamma}_r^T = \{ \hat{\gamma}_r^t, \hat{\gamma}_r^b, \hat{\gamma}_r^r, \hat{\gamma}_r^l, \hat{\gamma}_r^d, \hat{\gamma}_r^{-d}, \hat{\gamma}_r^a, \hat{\gamma}_r^{-a} \}^T. \quad (3)$$

The parametric space $\tilde{\gamma}$ (Section 2.2) is subsequently smooth out, rearranged into a vector and its dimensionality is reduced using the Karhunen-Loeve feature extraction ($\tilde{\gamma}$).

2.2 Illumination Invariant Textural Features

We assume that two images \tilde{Y}, Y of the same texture and view position differing only in illumination can be linearly transformed to each other:

$$\tilde{Y}_r = B Y_r,$$

where \tilde{Y}_r, Y_r are multispectral pixel values at position r and B is some transformation matrix dependent on an illumination. This linear formula is valid for changes in brightness and illumination spectrum, with surfaces including both Lambertian and specular reflectance. We have proven [20] that the following features are illumination invariant for each CAR model:

1. trace: $tr\{A_m^j\} \quad m = 1, \dots, \eta, j \in \{t, b, r, l, d, -d, a, -a\}$,
2. A_m eigenvalues: $\nu_{m,k}^j \quad k = 1, \dots, C$.

The illumination invariant feature vector (3) for every pixel r has the form:

$$\tilde{\gamma}_r^T = \left\{ tr\{A_1^t\}, \nu_{1,1}^t, \dots, \nu_{1,C}^t, \dots, tr\{A_\eta^{-a}\}, \dots, \nu_{\eta,1}^{-a}, \dots, \nu_{\eta,C}^{-a} \right\}^T. \quad (4)$$

2.3 Mixture Based Segmentation

Multi-spectral texture segmentation is done by clustering in the CAR parameter space Θ defined on the lattice I where

$$\Theta_r = [\bar{\gamma}_r, \zeta_r]^T \tag{5}$$

is the modified local parameter vector (3) computed for the lattice location r . The vector ζ_r contains both spatial coordinates r_1, r_2 and local colour values. We assume that this parametric space can be represented using the Gaussian mixture model (GM) with diagonal covariance matrices due to the previous CAR parametric space decorrelation. The Gaussian mixture model for CAR parametric representation at the m -th resolution ($m = 1, \dots, M$) is as follows:

$$p(\Theta_r^{(m)}) = \sum_{i=1}^{K^{(m)}} p_i^{(m)} p(\Theta_r^{(m)} | \nu_i^{(m)}, \Sigma_i^{(m)}) , \tag{6}$$

$$p(\Theta_r^{(m)} | \nu_i^{(m)}, \Sigma_i^{(m)}) = \frac{|\Sigma_i^{(m)}|^{-\frac{1}{2}}}{(2\pi)^{\frac{d}{2}}} e^{-\frac{(\Theta_r^{(m)} - \nu_i^{(m)})^T (\Sigma_i^{(m)})^{-1} (\Theta_r^{(m)} - \nu_i^{(m)})}{2}} . \tag{7}$$

The mixture model equations (6),(7) are solved using a modified EM algorithm.

Initialization. The algorithm is initialised using $\nu_i^{(m)}, \Sigma_i^{(m)}$ statistics for each resolution m estimated from the corresponding thematic maps in two subsequent steps:

1. refining direction
 $\nu_i^{(m-1)} \left(\forall \Theta_r^{(m-1)} : r \in \uparrow \Xi_i^{(m)} \right), \quad \Sigma_i^{(m-1)} \left(\forall \Theta_r^{(m-1)} : r \in \uparrow \Xi_i^{(m)} \right)$
 $m = M + 1, M, \dots, 2 \quad i = 1, \dots, K^{(m)} ,$
2. coarsening direction
 $\nu_i^{(m)} \left(\forall \Theta_r^{(m)} : r \in \downarrow \Xi_i^{(m-1)} \right), \quad \Sigma_i^{(m)} \left(\forall \Theta_r^{(m)} : r \in \downarrow \Xi_i^{(m-1)} \right)$
 $m = 2, 3, \dots, M \quad i = 1, \dots, K^{(m)} ,$

where $\Xi_i^{(m)} \subset I \forall m, i$, and the first initialisation thematic map $\Xi_i^{(M+1)}$ is approximated by the rectangular subimages obtained by regular division of the input texture mosaic. All the subsequent refining step are initialised from the preceding coarser resolution up-sampled thematic maps. The final initialisation results from the second coarsening direction where the gradually coarsening segmentations are initialised using the preceding down-sampled thematic maps. For each possible couple of components the Kullback-Leibler divergence

$$D(p(\Theta_r | \nu_i, \Sigma_i) || p(\Theta_r | \nu_j, \Sigma_j)) = \int_{\Omega} p(\Theta_r | \nu_i, \Sigma_i) \log \left(\frac{p(\Theta_r | \nu_i, \Sigma_i)}{p(\Theta_r | \nu_j, \Sigma_j)} \right) d\Theta_r$$

is evaluated and the most similar components, i.e.,

$$\{i, j\} = \arg \min_{k, l} D(p(\Theta_r | \nu_l, \Sigma_l) || p(\Theta_r | \nu_k, \Sigma_k))$$

are merged together in each initialisation step. This initialisation results in K_{ini} subimages and recomputed statistics ν_i, Σ_i . $K_{ini} > K$ where K is the optimal number of textured segments to be found by the algorithm. Two steps of the EM algorithm are repeating after initialisation. The components with smaller weights than a fixed threshold ($p_j < \frac{0.02}{K_{ini}}$) are eliminated. For every pair of components we estimate their Kullback-Leibler divergence. From the most similar couple, the component with the weight smaller than the threshold is merged to its stronger partner and all statistics are actualised using the EM algorithm. The algorithm stops when either the likelihood function has negligible increase ($\mathcal{L}_t - \mathcal{L}_{t-1} < 0.01$) or the maximum iteration number threshold is reached.

2.4 Resulting Mixture Probabilities

Resulting mixture model probabilities are mapped to the original fine resolution image space for all $m = 1, \dots, M$ mixture sub-models ((6)(7)). The M cooperating segmenters deliver their class response in the form of conditional probabilities. Each segmenter produces a preference list based on the mixture component probabilities of a particular pixel belonging a particular class, together with a set of confidence measurement values generated in the original decision-making process.

Single-Segmenters Correspondence. Single-resolution segmentation results cannot be combined without knowledge of the mutual correspondence between regions in all different-resolution segmentation probabilistic mixture component maps ($K^1 \times \sum_{m=2}^M K^m$ combinations). Mutual assignments of two probabilistic maps are solved by using the Munkre’s assignment algorithm [12] which finds the minimal cost assignment

$$g : A \mapsto B, \sum_{\alpha \in A} f(\alpha, g(\alpha))$$

between sets $A, B, |A| = |B| = n$ given the cost function $f(\alpha, \beta), \alpha \in A, \beta \in B$. α corresponds to the fine resolution probabilistic maps, β corresponds to down-sampled probabilistic maps and $f(\alpha, \beta)$ is the Kullback-Leibler divergence between probabilistic maps. The algorithm has polynomial complexity instead of exponential for the exhaustive search.

Final Parametric Space. The parametric vectors representing texture mosaic pixels are assigned to the clusters based on our modification of the sum rule according to the highest component probabilities, i.e., Y_r is assigned to the cluster ω_{j^*} if [9]

$$\pi_{r,j^*} = \max_j \sum_{s \in I_r} w_s \left(\sum_{m=1}^M \frac{p^2(\Theta_{r-s}^{(m)} | \nu_j^{(m)}, \Sigma_j^{(m)})}{\sum_{i=1}^M p(\Theta_{r-s}^{(i)} | \nu_j^{(i)}, \Sigma_j^{(i)})} \right),$$

where w_s are fixed distance-based weights, I_r is a rectangular neighbourhood and $\pi_{r,j^*} > \pi_{thre}$ (otherwise the pixel is unclassified). The area of single cluster blobs is evaluated in the post-processing thematic map filtration step. Regions with similar statistics are merged. Thematic map blobs with area smaller than a given threshold are attached to its neighbour with the highest similarity value.

3 Experimental Results

The algorithm was tested on natural wooden bidirectional texture function (BTF) mosaics from the Prague Texture Segmentation Data-Generator and Benchmark (<http://mosaic.utia.cas.cz>) [6]. The benchmark test mosaics layouts and each cell texture membership are randomly generated and filled with BTF textures from the large UTIA BTF database. The BTF wood measurements are mapped on the randomly generated spline surface. These tested BTFs have 3 spectral bands ($d = 3$) but the segmenter can handle any number of bands.

The benchmark ranks segmentation algorithms according to a chosen criterion. There are implemented twenty seven most frequented evaluation criteria categorised into four criteria groups – region-based [6], pixel-wise [6], clustering comparison criteria, and consistency measures [6]. The region-based [6] performance criteria mutually compare ground truth (GT) image regions with the corresponding machine segmented regions (MS). The pixel-wise criteria group contains the most frequented classification criteria such as the omission and commission errors, class accuracy, recall, precision, etc. Finally the last two criteria sets incorporate the global and local consistency errors [6] and three clustering comparison criteria.

Table 1 compares the overall benchmark performance of the proposed algorithm MW3AR8ⁱ with the Voting Representativeness - Priority Multi-Class Flooding Algorithm (VRA-PMCFA) [8,16], Segmentation by Weighted Aggregation (SWA) [19], Efficient Graph-Based Image Segmentation (EGBIS) [3], Factorization-based texture SEGmenter (FSEG) [21], HGS [13], Edge Detection and Image SegmentatiON (EDISON) [1], JSEG [2], Deep Brain Model (DBM) [8], respectively. The table criteria are averaged over 10 experimental mosaics.

MW3AR8ⁱ ranks second (average rank 3.05) over all benchmark criteria, slightly worse than the overall winner of the ICPR 2014 Unsupervised Image Segmentation Contest [8] - the VRA-PMCFA method.

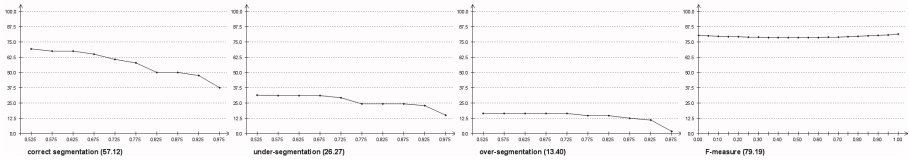
These results illustrated in Figs. 1-3 and Table 1 demonstrate very good pixel-wise, correct region segmentation, missed error, noise error, and undersegmentation properties of our method. For most the pixel-wise criteria our method is among the best ones while. Our oversegmentation value is the second worst from all the compared methods what offers a large space for further improvement by better future post-processing.

Figs. 2,3 and show five selected 1024×1024 experimental benchmark mosaics created from four to twelve natural BTF textures. The last four or five rows on these figures demonstrate comparative results from the eight alternative algorithms. Three methods (VRA-PMCFA, FSEG, DBM) participated in the ICPR contest.

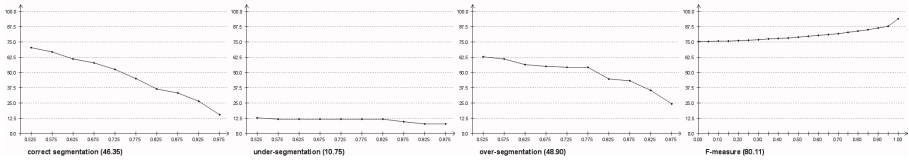
Table 1. BTF wood benchmark results for VRA-PMCFA, MW3AR8^z, SWA, EGBIS, FSEG, HGS, EDISON, JSEG, DBM. (Benchmark criteria: CS = correct segmentation; OS = over-segmentation; US = under-segmentation; ME = missed error; NE = noise error; O = omission error; C = commission error; CA = class accuracy; CO = recall - correct assignment; CC = precision - object accuracy; I. = type I error; II. = type II error; EA = mean class accuracy estimate; MS = mapping score; RM = root mean square proportion estimation error; CI = comparison index; GCE = Global Consistency Error; LCE = Local Consistency Error; dD = Van Dongen metric; dM = Mirkin metric; dVI = variation of information; \bar{f} are the performance curves integrals; \bar{F} = F-measure curve; small numbers are the corresponding measure rank over the listed methods.)

	VRA-PMCFA (2.19)	MW3-AR8 ^z (3.05)	SWA (3.33)	EGBIS (4.90)	FSEG (5.14)	HGS (5.38)	EDISON (6.14)	JSEG (7.19)	DBM (7.67)
↑ CS	59.55 ¹	49.78 ²	44.87 ⁴	45.41 ³	36.87 ⁶	42.79 ⁵	29.25 ⁷	20.15 ⁸	17.86 ⁹
↓ OS	16.10 ²	53.96 ⁸	19.97 ⁵	34.19 ⁷	58.03 ⁹	11.92 ¹	19.68 ⁴	17.83 ³	23.80 ⁶
↓ US	29.22 ⁵	11.58 ²	26.60 ³	45.90 ⁷	10.31 ¹	30.01 ⁶	61.32 ⁸	27.53 ⁴	62.59 ⁹
↓ ME	6.00 ³	4.51 ²	8.76 ⁶	1.13 ¹	9.36 ⁷	23.62 ⁸	8.20 ⁵	40.30 ⁹	8.06 ⁴
↓ NE	6.33 ³	4.90 ²	9.15 ⁵	2.81 ¹	9.52 ⁷	26.06 ⁸	8.10 ⁴	38.68 ⁹	9.49 ⁶
↓ O	16.15 ³	12.87 ²	12.79 ¹	35.79 ⁶	26.86 ⁵	23.34 ⁴	49.92 ⁸	47.89 ⁷	70.86 ⁹
↓ C	16.98 ¹	91.10 ⁶	30.30 ²	96.43 ⁸	91.47 ⁷	40.85 ³	90.00 ⁴	100.00 ⁹	90.33 ⁵
↑ CA	72.28 ¹	70.07 ²	68.01 ³	57.47 ⁶	59.75 ⁵	59.83 ⁴	45.29 ⁷	45.08 ⁸	36.39 ⁹
↑ CO	80.25 ¹	75.02 ³	75.61 ²	68.06 ⁵	64.74 ⁶	71.29 ⁴	60.40 ⁷	57.99 ⁸	52.64 ⁹
↑ CC	81.30 ³	93.72 ¹	80.28 ⁴	78.42 ⁵	91.07 ²	72.97 ⁷	72.74 ⁸	75.16 ⁶	55.90 ⁹
↓ I.	19.75 ¹	24.98 ³	24.39 ²	31.94 ⁵	35.26 ⁶	28.71 ⁴	39.60 ⁷	42.01 ⁸	47.36 ⁹
↓ II.	2.78 ²	3.25 ⁴	3.07 ³	8.22 ⁶	1.51 ¹	6.21 ⁵	15.38 ⁹	9.28 ⁷	14.99 ⁸
↑ EA	78.35 ²	78.71 ¹	75.08 ³	63.05 ⁶	71.04 ⁴	69.24 ⁵	51.74 ⁸	55.19 ⁷	44.70 ⁹
↑ MS	73.17 ¹	70.92 ²	66.63 ³	54.77 ⁶	60.04 ⁴	59.77 ⁵	41.81 ⁸	42.56 ⁷	32.19 ⁹
↓ RM	6.37 ⁴	4.09 ¹	5.76 ³	6.83 ⁶	4.37 ²	7.09 ⁷	8.47 ⁸	6.53 ⁵	11.83 ⁹
↑ CI	79.51 ²	80.56 ¹	76.46 ³	66.14 ⁶	74.19 ⁴	70.54 ⁵	54.98 ⁸	59.16 ⁷	47.92 ⁹
↓ GCE	6.27 ¹	7.20 ³	9.50 ⁵	8.46 ⁴	13.41 ⁷	19.74 ⁸	6.77 ²	23.23 ⁹	12.72 ⁶
↓ LCE	3.77 ⁴	4.38 ⁵	3.52 ³	2.85 ²	7.44 ⁶	14.02 ⁹	1.92 ¹	12.20 ⁸	7.58 ⁷
↓ dD	11.45 ¹	14.21 ³	13.82 ²	16.81 ⁴	20.41 ⁶	19.06 ⁵	20.90 ⁷	25.05 ⁸	26.01 ⁹
↓ dM	7.75 ¹	10.16 ³	8.79 ²	20.33 ⁶	12.27 ⁴	12.34 ⁵	30.58 ⁸	20.98 ⁷	33.07 ⁹
↓ dVI	14.53 ⁴	16.56 ⁸	14.87 ⁶	13.97 ³	18.29 ⁹	14.85 ⁵	12.66 ¹	15.51 ⁷	13.57 ²
↑ \overline{CS}	57.12 ¹	46.35 ³	49.84 ²	44.89 ⁴	32.85 ⁶	37.65 ⁵	29.48 ⁷	22.94 ⁸	16.37 ⁹
↓ \overline{OS}	13.40 ¹	48.90 ⁸	20.55 ⁴	36.41 ⁷	51.65 ⁹	14.32 ²	22.22 ⁶	21.11 ⁵	20.33 ³
↓ \overline{US}	26.27 ⁶	10.75 ²	24.26 ⁴	36.16 ⁷	8.27 ¹	25.92 ⁵	57.14 ⁹	23.92 ³	53.86 ⁸
↓ \overline{ME}	11.91 ²	13.97 ⁵	13.14 ⁴	12.16 ³	21.50 ⁶	33.95 ⁸	11.59 ¹	42.40 ⁹	22.36 ⁷
↓ \overline{NE}	11.89 ²	14.04 ⁵	13.07 ³	13.39 ⁴	21.94 ⁶	35.50 ⁸	11.83 ¹	41.59 ⁹	24.00 ⁷
↑ \overline{F}	79.19 ²	80.11 ¹	76.07 ³	65.22 ⁶	73.28 ⁴	70.17 ⁵	54.34 ⁸	57.95 ⁷	47.00 ⁹

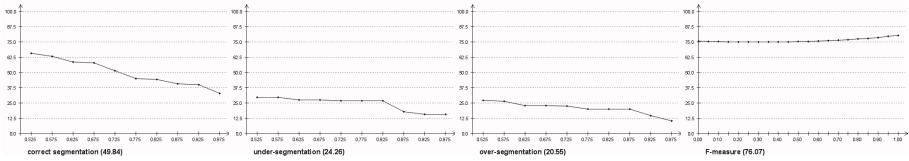
VRA-PMCFA



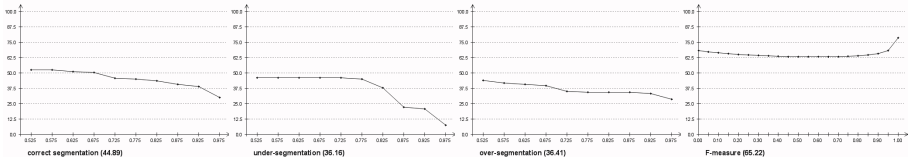
MW3AR8²



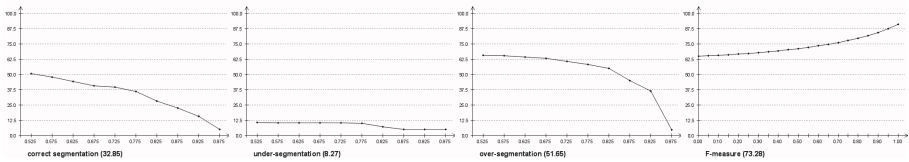
SWA



EGBIS



FSEG



HGS

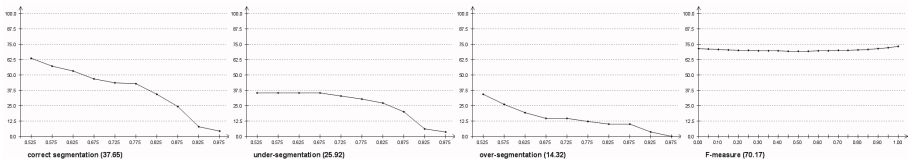


Fig. 1. Performance curves (vertical axis - $f(threshold)$, horizontal axis - threshold, details in <http://mosaic.utia.cas.cz>) of correct segmentation, undersegmentation, over-segmentation, and F-measure, respectively.

BTF mosaic



ground truth



VRA-PMCEFA

MW3-AR8ⁱ

SWA



EGBIS

**Fig. 2.** BTF mosaic, ground truth, and segmentation results, respectively.

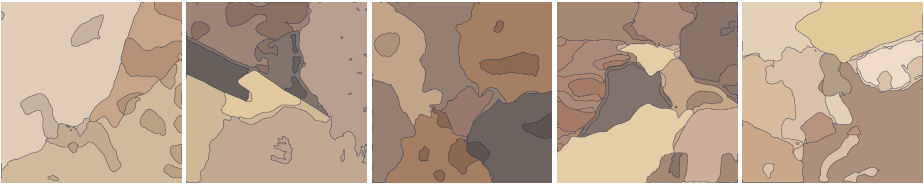
ground truth



FSEG



HGS



EDISON



JSEG



DBM



Fig. 3. Ground truth, and segmentation results, respectively.

The contest used the large size (80 textural mosaics) unsupervised *Colour* benchmark without noise degradation and with linear region borders. The contest criterion was the average rank over all benchmark criteria.

Hard natural BTF textures were chosen rather than synthesised (for example using Markov random field models) ones because they are expected to be more difficult for the underlying segmentation model. The fourth row on Fig. 2 demonstrates solid behaviour of our MW3AR8ⁱ algorithm but also infrequent algorithm failures producing the oversegmented thematic map for some textures. Such failures can be reduced by a more elaborate post-processing step.

The SWA [19], EGBIS [3], FSEG [21], HGS [13], EDISON [1], JSEG [2], and DBM algorithms on these data performed mostly worse as can be seen in their corresponding rows on Figs. 2,3 some areas are undersegmented while other parts of the mosaics are oversegmented. The best six method's performance is illustrated also on Fig. 1.

4 Conclusions

We proposed a significant improvement of our previously published unsupervised multi-segmenter [9]. The MW3AR8ⁱ segmenter is computationally efficient and robust method for unsupervised textured image segmentation with unknown number of classes based on the underlying CAR and GM texture models. The algorithm is reasonably fast, despite of using the random field type data representation, due to its efficient recursive parameter estimation of the underlying models and therefore is much faster than the usual Markov chain Monte Carlo estimation approach required for the Markovian image representations. Usual drawback of most segmentation methods is their application dependent parameters to be experimentally estimated. Our method requires only a contextual neighbourhood selection and two additional thresholds. The method's performance is demonstrated on the extensive benchmark tests on both natural texture mosaics as well as on BTF mosaics. It performs favourably compared with eight alternative segmentation algorithms. Detailed experimental results are available in <http://mosaic.utia.cas.cz>.

Acknowledgments. This research was supported by the Czech Science Foundation project GAČR 14-10911S.

References

1. Christoudias, C., Georgescu, B., Meer, P.: Synergism in low level vision. In: Kasturi, R., Laurendeau, D., Suen, C. (eds.) Proceedings of the 16th International Conference on Pattern Recognition, vol. 4, pp. 150–155. IEEE Computer Society, Los Alamitos (2002)
2. Deng, Y., Manjunath, B.: Unsupervised segmentation of color-texture regions in images and video. IEEE Transactions on Pattern Analysis and Machine Intelligence **23**(8), 800–810 (2001)

3. Felzenszwalb, P., Huttenlocher, D.: Efficient graph-based image segmentation. *IJCV* **59**(2), 167–181 (2004)
4. Haindl, M.: Texture synthesis. *CWI Quarterly* **4**(4), 305–331 (1991)
5. Haindl, M., Mikeš, S.: Unsupervised texture segmentation using multispectral modelling approach. In: Tang, Y., Wang, S., Yeung, D., Yan, H., Lorette, G. (eds.) *Proceedings of the 18th International Conference on Pattern Recognition, ICPR 2006*, vol. II, pp. 203–206. IEEE Computer Society, Los Alamitos (2006)
6. Haindl, M., Mikeš, S.: Texture segmentation benchmark. In: Lovell, B., Laurendeau, D., Duin, R. (eds.) *Proceedings of the 19th International Conference on Pattern Recognition, ICPR 2008*, pp. 1–4. IEEE Computer Society, Los Alamitos (2008)
7. Haindl, M., Mikeš, S.: Model-based texture segmentation. In: Campilho, A.C., Kamel, M.S. (eds.) *ICIAR 2004*. LNCS, vol. 3212, pp. 306–313. Springer, Heidelberg (2004)
8. Haindl, M., Mikeš, S.: Unsupervised image segmentation contest. In: *Proceedings of the 22nd International Conference on Pattern Recognition, ICPR 2014*, pp. 1484–1489. IEEE Computer Society CPS, Los Alamitos, August 2014. <http://mosaic.utia.cas.cz/icpr2014/>
9. Haindl, M., Mikeš, S., Pudil, P.: Unsupervised hierarchical weighted multi-segmenter. In: Benediktsson, J.A., Kittler, J., Roli, F. (eds.) *MCS 2009*. LNCS, vol. 5519, pp. 272–282. Springer, Heidelberg (2009)
10. Haindl, M.: Texture segmentation using recursive Markov random field parameter estimation. In: Bjarne, K.E., Peter, J. (eds.) *Proceedings of the 11th Scandinavian Conference on Image Analysis*, pp. 771–776. Pattern Recognition Society of Denmark, Lyngby (1999)
11. Haindl, M.: Visual data recognition and modeling based on local markovian models. In: Florack, L., Duits, R., Jongbloed, G., Lieshout, M.C., Davies, L. (eds.) *Mathematical Methods for Signal and Image Analysis and Representation, Computational Imaging and Vision*, chap. 14, vol. 41, pp. 241–259. Springer, London (2012). doi:[10.1007/978-1-4471-2353-8_14](https://doi.org/10.1007/978-1-4471-2353-8_14)
12. Haindl, M., Mikeš, S.: Unsupervised texture segmentation using multiple segmenters strategy. In: Haindl, M., Kittler, J., Roli, F. (eds.) *MCS 2007*. LNCS, vol. 4472, pp. 210–219. Springer, Heidelberg (2007)
13. Hoang, M.A., Geusebroek, J.M., Smeulders, A.W.: Color texture measurement and segmentation. *Signal Processing* **85**(2), 265–275 (2005)
14. Kittler, J., Hojjatoleslami, A., Windeatt, T.: Weighting factors in multiple expert fusion. In: *Proc. BMVC*, pp. 41–50. BMVA (1997)
15. Manjunath, B., Chellapa, R.: Unsupervised texture segmentation using markov random field models. *IEEE Transactions on Pattern Analysis and Machine Intelligence* **13**, 478–482 (1991)
16. Panagiotakis, C., Grinias, I., Tziritas, G.: Natural image segmentation based on tree equipartition, bayesian flooding and region merging. *IEEE Transactions on Image Processing* **20**(8), 2276–2287 (2011)
17. Panjwani, D., Healey, G.: Markov random field models for unsupervised segmentation of textured color images. *IEEE Transactions on Pattern Analysis and Machine Intelligence* **17**(10), 939–954 (1995)

18. Reed, T.R., du Buf, J.M.H.: A review of recent texture segmentation and feature extraction techniques. *CVGIP-Image Understanding* **57**(3), 359–372 (1993)
19. Sharon, E., Galun, M., Sharon, D., Basri, R., Brandt, A.: Hierarchy and adaptivity in segmenting visual scenes. *Nature* **442**(7104), 719–846 (2006)
20. Vacha, P., Haindl, M.: Image retrieval measures based on illumination invariant textural mrf features. In: *CIVR 2007: Proceedings of the 6th ACM international conference on Image and video retrieval*, pp. 448–454. ACM Press, New York (2007)
21. Yuan, J., Wang, D.: Factorization-based texture segmentation. Tech. Rep. OSU-CISRC-1/13-TR0, The Ohio State University, Columbus (2013)